CORRELATION OF ANALYTICAL AND EXPERIMENTAL RESULTS OF CYLINDRICAL SHELLS UNDER NEWTONIAN PRESSURE DISTRIBUTION

by

Nicholas C. Lycurgus*
and
Wesley R. Midgley**

30 April 1965

Tests were performed to determine whether or not linear extensional shell theory is applicable to the analysis of cylindrical shells constructed of unfurlable wire cloth material and subjected to Newtonian type pressure distribution. Since the objective was to compare test results with results obtained through the application of linear extensional shell theory, the analysis and testing were performed on a stainless steel foil shell, which eliminated the problem of non-isotropy of the wire cloth material. It is expected that a similar comparison will be performed at a later date using wire cloth.

The comparison of analytical with test results, as well as the analytical results themselves, shows that linear extensional shell theory is applicable to the analysis of steel foil cylindrical shells under Newtonian pressure distribution.

* Assistant to the Chief, Analytical Mechanics
Avco Research and Advanced Development Division, Wilmington, Mass.

** Staff Engineer, Structures Laboratory
Avco Research and Advanced Development Division, Wilmington, Mass.

I. INTRODUCTION

In the course of determining the feasibility of designing and manufacturing primary structural components in the area of advanced reenty vehicles partially constructed of unfurlable materials, investigations were conducted to assure that approximate analytical methods involving the application of linear extensional shell theory could be used in the design of this type of structures subjected to nonsymmetrical surface loadings. To demonstrate this, experimental tests were performed on a right circular cylindrical shell of stainless steel foil subjected to a normal loading of the form A+B cos β. This was imposed through the use of liquid mercury by filling the shell completely and later on subjecting it to additional internal pressure. This type of loading simulates exactly the first two terms of a nonsymmetrical Newtonian Pressure Distribution, the difference existing only in the absolute values of the constants A and B.

This paper presents, first, the experimental testing performed on the cylindrical shell, second, the analytical procedure followed in the prediction of the quantities under consideration and third, a comparison of the experimental results obtained with the theoretical conclusions.

1. Experimental Testing

A 0.010-inch-thick, longitudinally welded, type 304 stainless-steel cylindrical shell having a modulus of elasticity $E = 25.9 \times 10^6$ psi average of 2 specimens with maximum error about $\pm 2.8 \times 10^6$ psi, and a Poisson's Ratio $\nu = 0.3$ was sealed at its ends and supported as shown in the schematic of the test setup of figure 1. The inner diameter was measured to be 19.8 inches, and the length between attached end plates 20.2 inches. The metal end-plates were counter weighted before the application of any loading, to remove any end force system they could impart to the shell before testing. At midlength of the shell, LVDT's (linearly variable differential transformers) were installed to measure displacement of the cross section and one quarter inch away from midlength, foil strain gages (type FAB-25-12) were installed to measure strains. Sections BB and CC of figure 1 show schematically the LVDT's and strain gages respectively. Figure 2 shows the cylindrical shell during installation. The instrumentation, is readily discernable in this photograph.

The cylinder was first filled and pressurized with water to locate any leaks, and also to preload the cylinder to yield local areas where residual stress might be high or where stress concentrations exist. About six small leaks were located, the water drained, and the holes repaired by bonding stainless steel shim stock over the full length of the weld bead with a room temperature vulcanizing rubber compound. The cylinder was then filled to depths of 4, 10, 15, and 19.8 inches, that is completely filled with mercury having

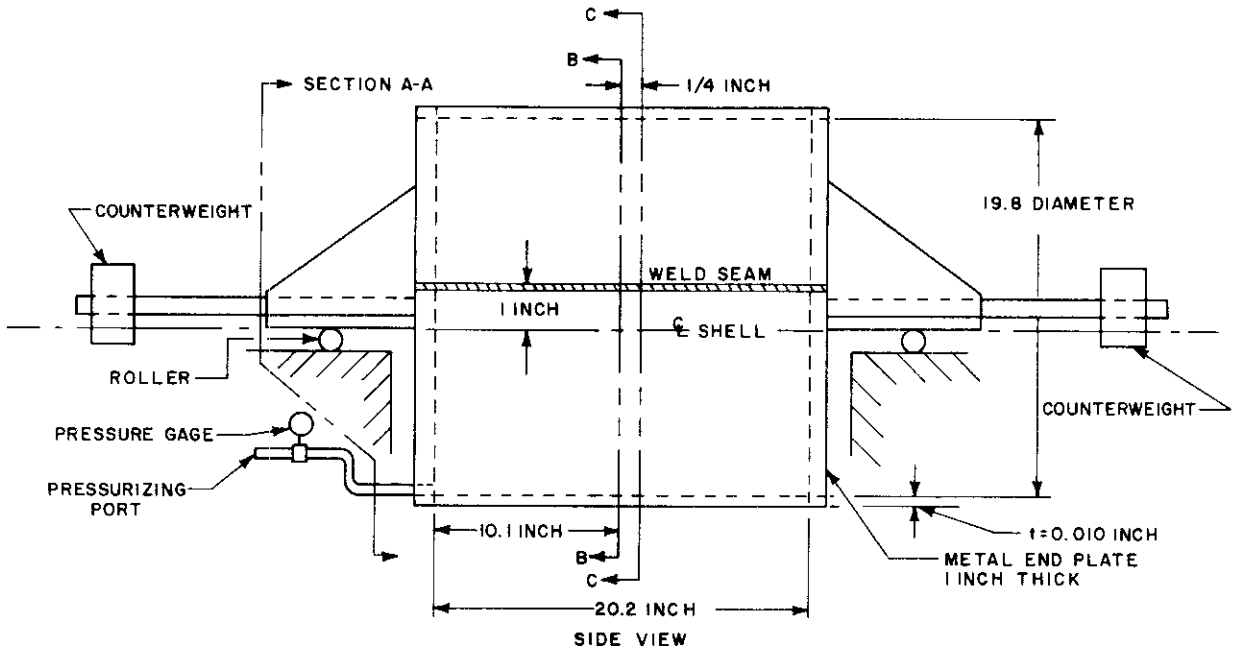

NOTE: COUNTERWEIGHT BALANCED BEFORE FILLING CYLINDER WITH MERCURY

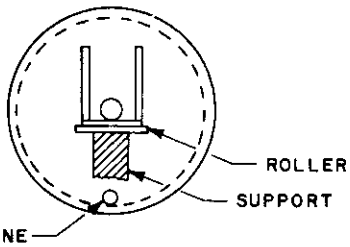

SECTION A-A SHOWING CYLINDER SUPPORT

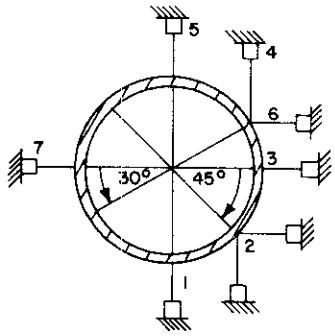

SECTION B-B SHOWING LOCATION OF LVDT'S

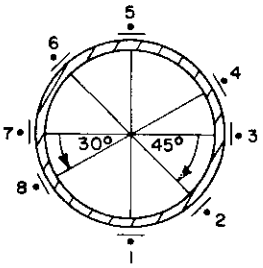

INDICATES TWO TYPE FAB-25-12 FOIL STRAIN GAGES

SECTION C-C SHOWING LOCATION OF STRAIN GAGES

65-5311

Figure 1 TEST SETUP FOR STAINLESS STEEL CYLINDRICAL SHELL

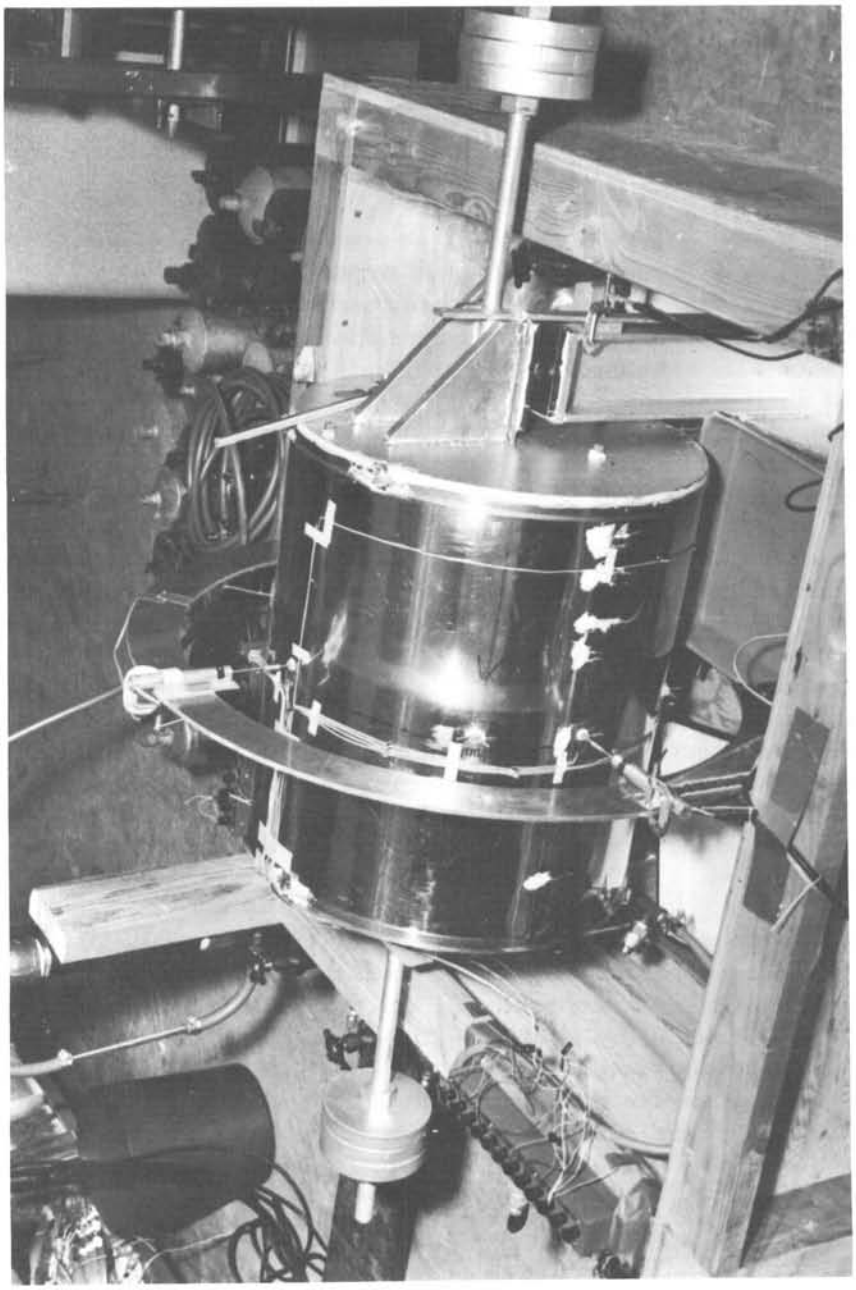

Figure 2 TEST SETUP DURING INSTALLATION OF INSTRUMENTATION

a density of $\gamma = 0.492$ lb/in.^{3} Deformations and strains were recorded at each depth of mercury. The shell was then pressurized to 8.8, 13.6, 18.4, 22.8, 0, 22.8, 28.2, and 0 psi. The load imposed by the liquid mercury together with the additional induced pressure simulated the first two terms, $A + B \cos \beta$, of a non-symmetric Newtonian Pressure Distribution. Figure 3 is a close-up view showing the instrumentation during the test. Deformations and strains were recorded for each LVDT and strain gage, at each loading condition.

It is interesting to note the deformations, shown in figure 4, of the cross section at midlength of the shell at different depths of mercury. At a depth of 10 inches of mercury, the shell deformed inwardly at the neutral axis of the cross section, and at a depth of 15 inches the deformation in the same direction at about 4 inches above the neutral axis of the cross section. When the cylindrical shell was completely filled with mercury and at 0 psi additional pressure, the cross section was close to the expected shape. At maximum pressurization, the maximum deformation was about 0.016 inch at the bottom of the cylindrical shell at LVDT gage 1.

Figure 5 shows plots of uniform internal pressure versus longitudinal and circumferential strains for gages 1, 5, and 3, 7 (this figure does not include strains due to hydrostatic head of mercury). As shown in figure 1, gages 1 and 5 are located at the bottom and top of the shell respectively and gages 3 and 7 on each side at the neutral axis. It is obvious from the plots that the structure behaved linearly and that the gages functioned properly. If the structure was perfectly symmetrical and the gages placed symmetrically, then, of course, the plots of the circumferential and longitudinal strains of gages 3 and 7, and 1 and 5 would be of the same magnitude. The maximum strain occurred in the circumferential direction and was about 800 microinches per inch tension.

Figures 6 and 7 show plots of pressure versus circumferential and longitudinal strains respectively of the cross section of the shell at midlength, including the hydrostatic head of mercury. The local effect of the weld seam is much more predominant in the longitudinal-strain plot than in the circumferential. The reason is probably due to the effect of the larger cross sectional area of the weld in the longitudinal direction, the weld bead not being ground off. The maximum circumferential strain shown in figure 6 was about 1250 microinches per inch tension, and the maximum longitudinal strain of figure 7 about 340 microinches per inch tension.

2. Analytical Procedure

The analysis of the test specimen was based on the approximate extensional theory of cylindrical shells. The field equations of cylindrical shells, as established in reference 1, are used to arrive at the equations of the extensional theory which then are solved explicitly for an arbitrary normal load

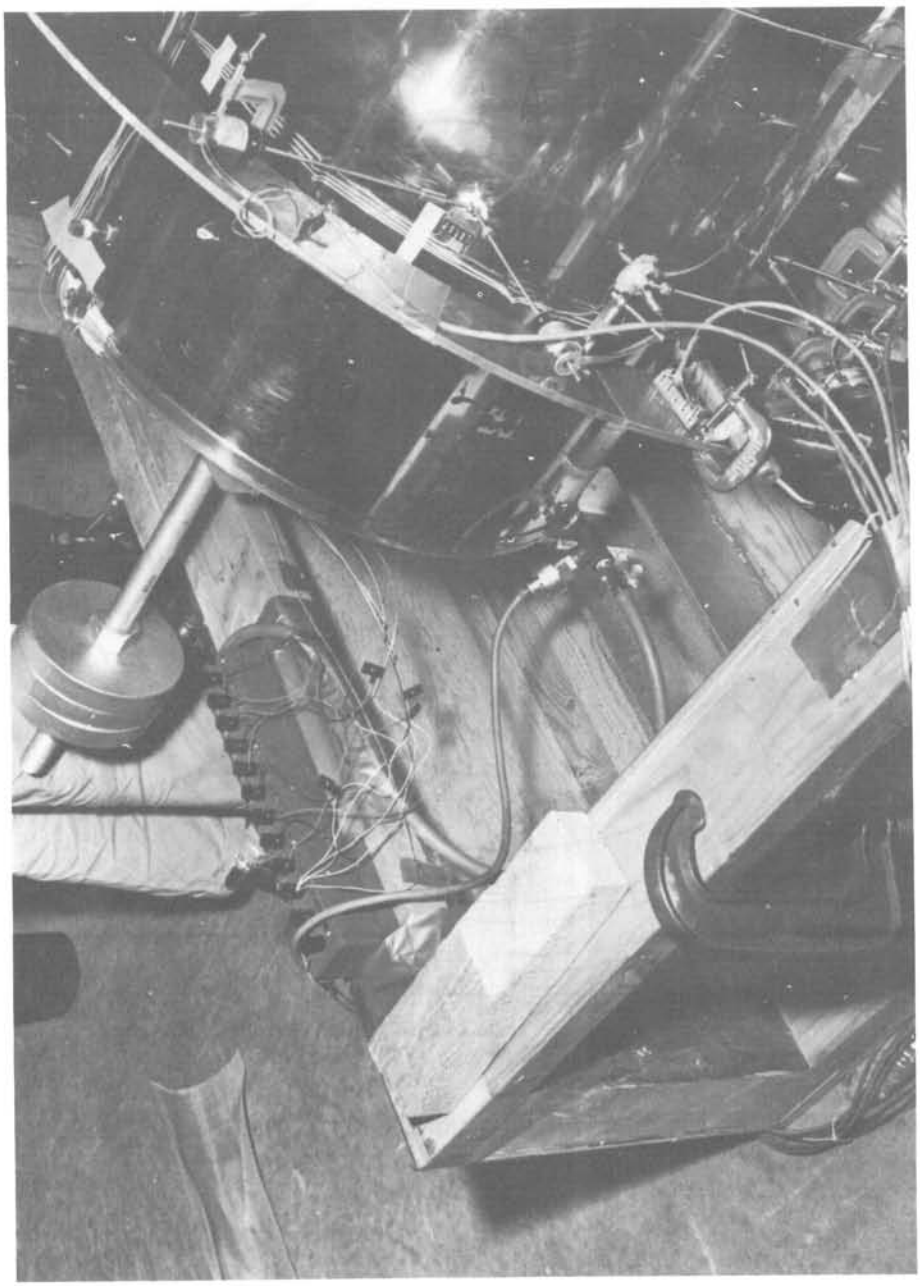

Figure 3 CLOSE-UP VIEW OF INSTRUMENTATION DURING TESTING

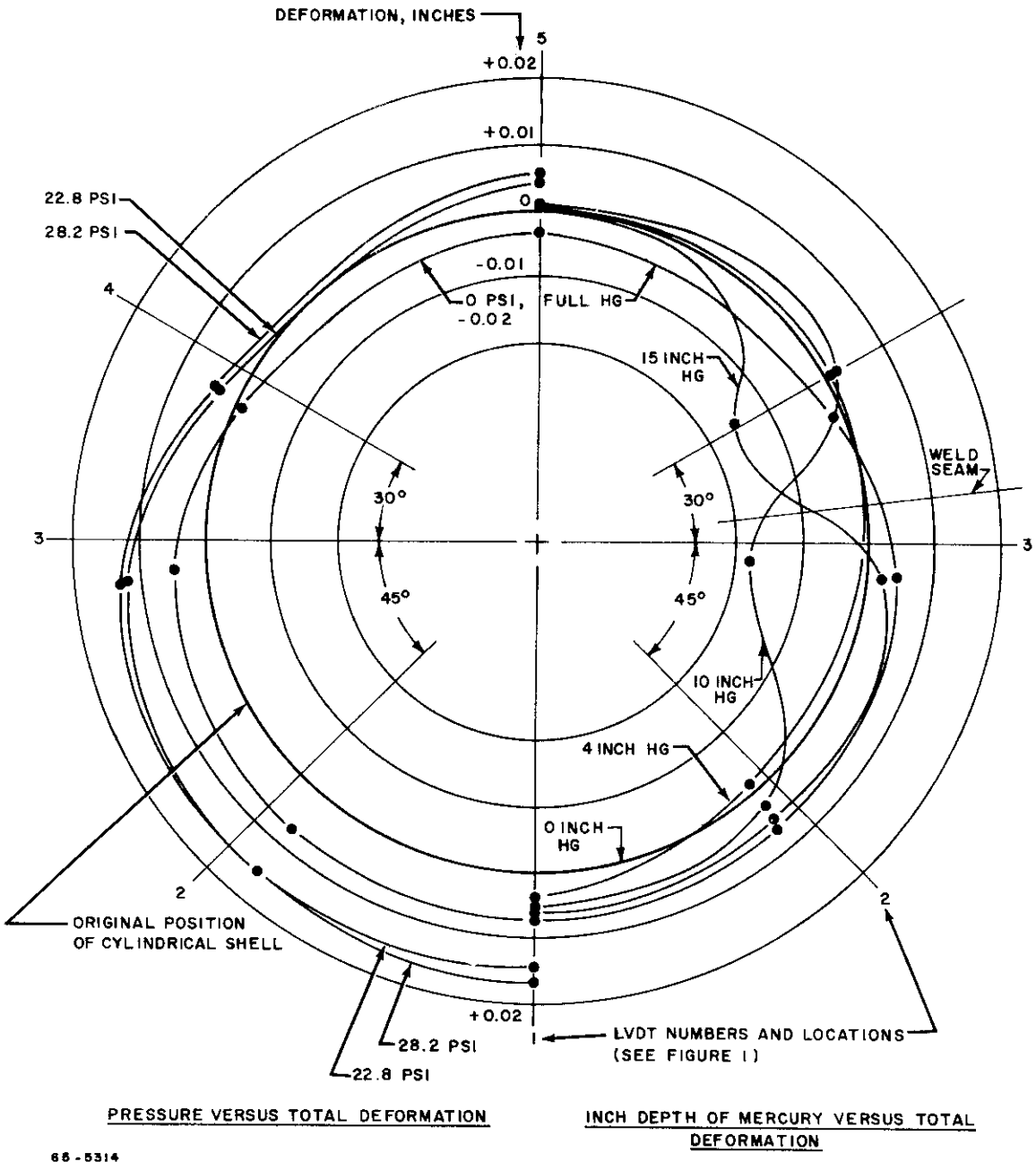

Figure 4 TOTAL DEFORMATION OF CROSS SECTION AT MIDLENGTH OF CYLINDRICAL SHELL

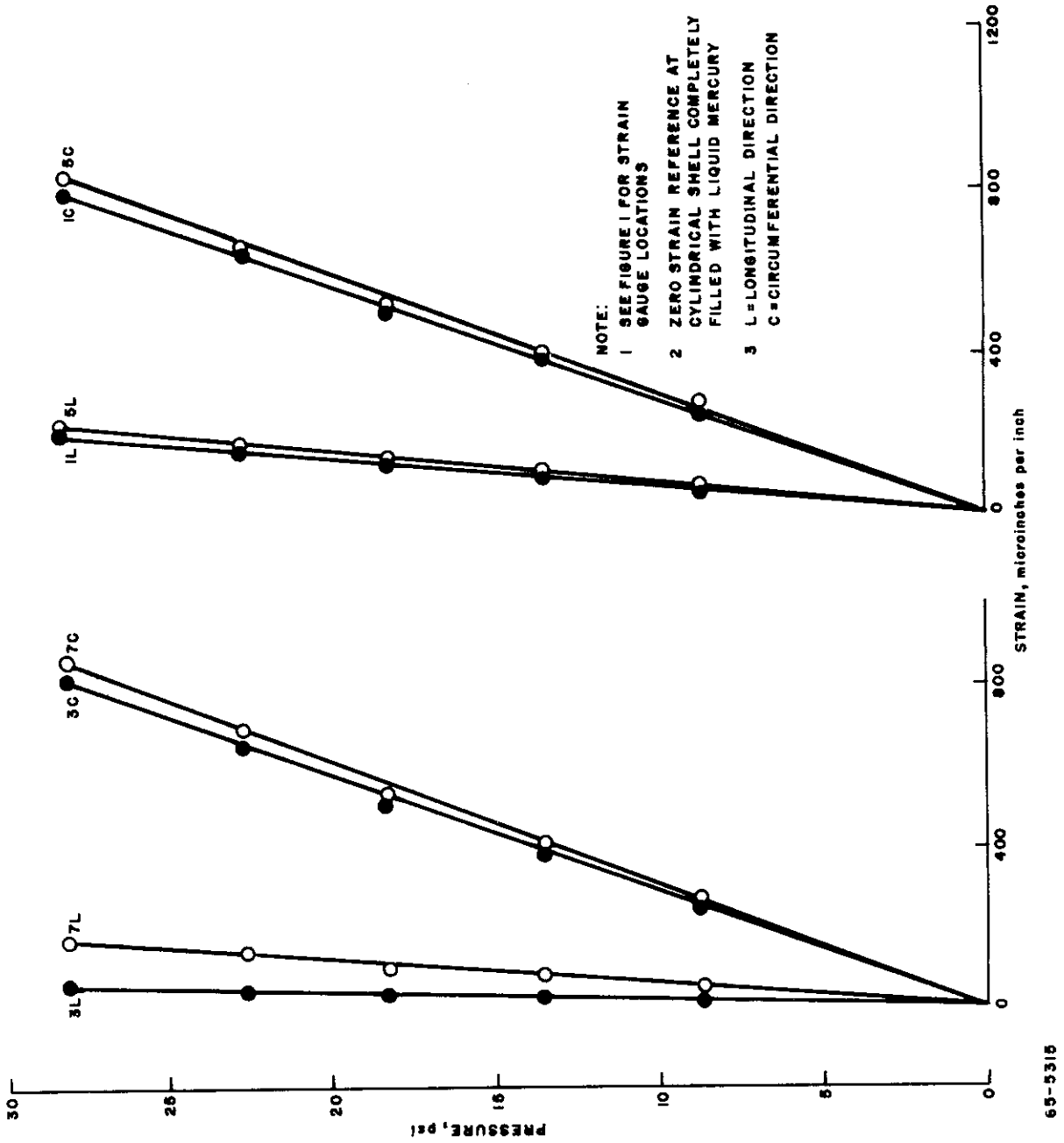

Figure 5 PRESSURE VERSUS STRAIN FOR GAGE LOCATIONS 1, 5 AND 3, 7

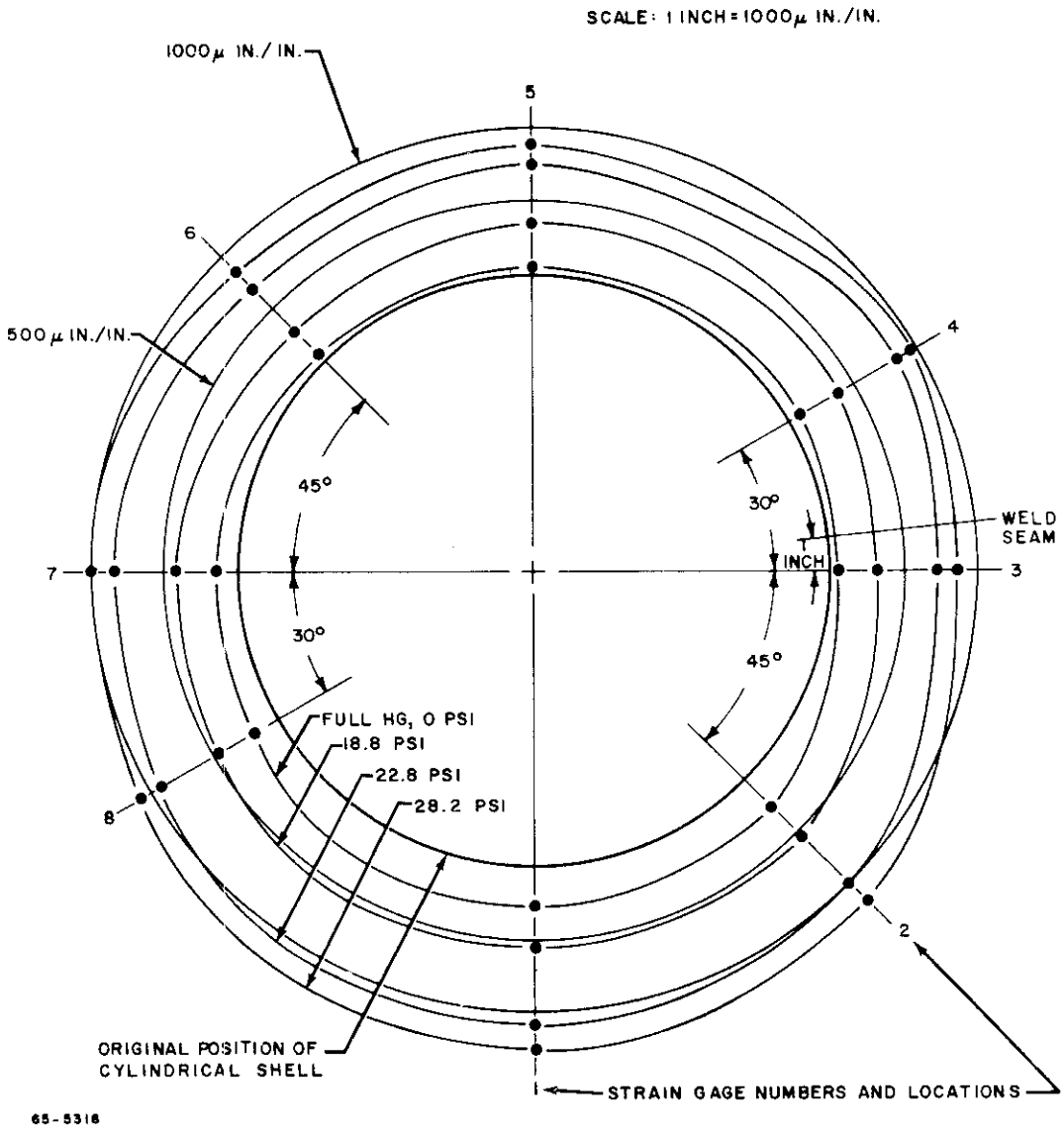

Figure 6 PRESSURE VERSUS CIRCUMFERENTIAL STRAIN OF THE CROSS SECTION AT MIDLENGTH OF THE CYLINDRICAL SHELL

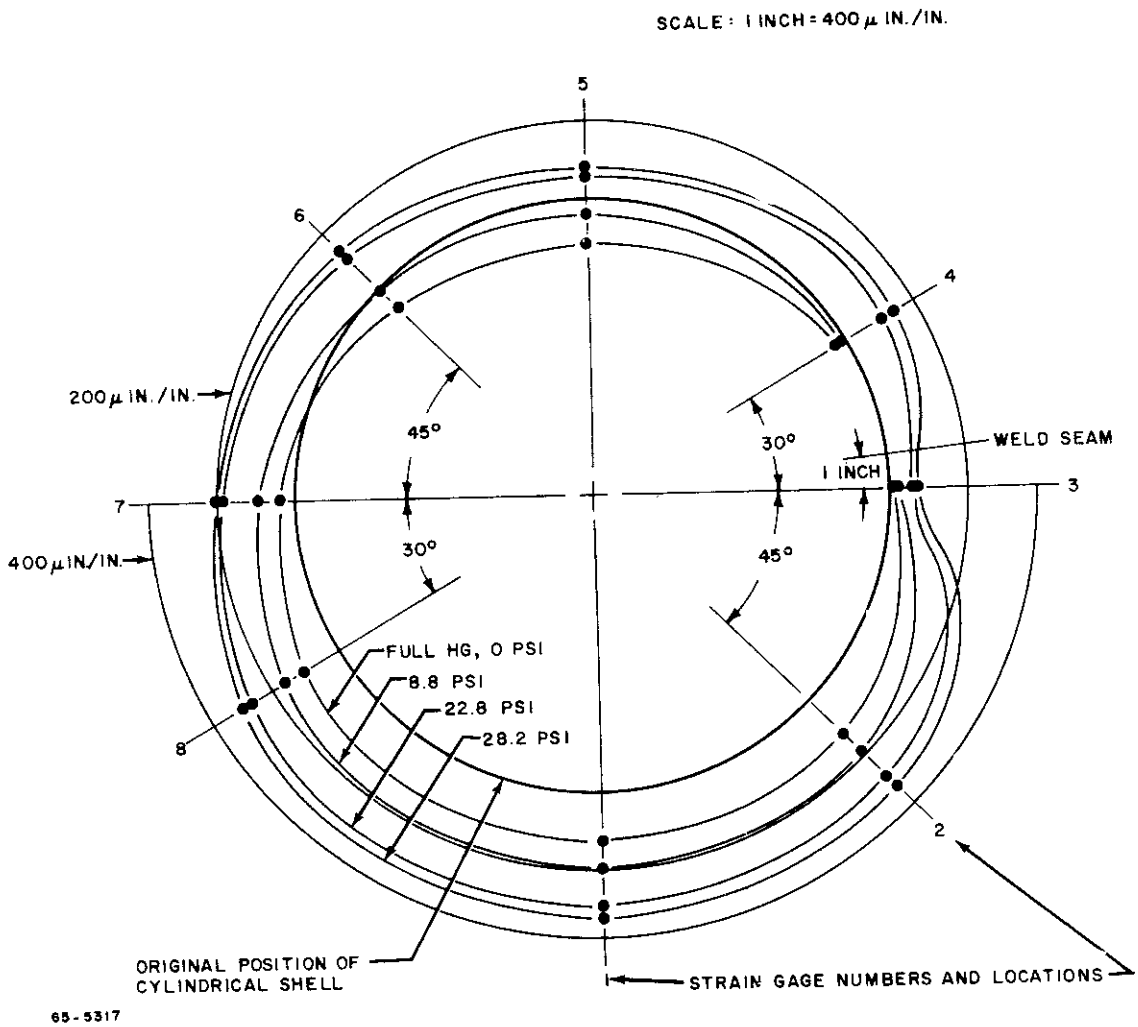

Figure 7 PRESSURE VERSUS LONGITUDINAL STRAIN OF THE CROSS SECTION AT MIDLENGTH OF THE CYLINDRICAL SHELL

$$S_1 + S_2 + \frac{H_2}{R} = 0$$

Strain-Displacement Equations

$$\epsilon_1 = \frac{\partial u}{\partial a}$$

$$\epsilon_2 = \frac{1}{R}\left(\frac{\partial v}{\partial \beta} - w\right)$$

$$\epsilon_{12} = \frac{1}{R}\frac{\partial u}{\partial \beta} + \frac{\partial v}{\partial a}$$

$$\kappa_1 = \frac{\partial^2 w}{\partial a^2}$$

$$\kappa_2 = \frac{1}{R^2}\left(\frac{\partial^2 w}{\partial \beta^2} + \frac{\partial v}{\partial \beta}\right)$$

$$\kappa_{12} = \frac{1}{R}\left(\frac{\partial^2 w}{\partial a\, \partial \beta} + \frac{\partial v}{\partial a}\right)$$

Stress-Strain Relations

$$T_1 = \frac{Et}{1-\nu^2}(\epsilon_1 + \nu\epsilon_2)$$

$$T_2 = \frac{Et}{1-\nu^2}(\epsilon_2 + \nu\epsilon_1)$$

$$S_1 = \frac{Et}{2(1+\nu)}\left(\epsilon_{12} + \frac{t^2\kappa_{12}}{6R}\right)$$

$$S_2 = -\frac{Et}{2(1+\nu)}(\epsilon_{12})$$

$$G_1 = -\frac{Et^3}{12(1-\nu^2)}(\kappa_1 + \nu\kappa_2)$$

$$G_2 = -\frac{Et^3}{12(1-\nu^2)}(\kappa_2 + \nu\kappa_1)$$

$$H_1 = \frac{Et^3}{12(1+\nu)}(\kappa_{12})$$

$$H_2 = -\frac{Et^3}{12(1+\nu)}(\kappa_{12})$$

It can be easily seen that the 6th equilibrium equation is an identity, leaving a system of 19 equations in 19 unknowns.

The elimination of the transverse shears N_1, N_2, and their derivatives from the first three equilibrium equations, and the deletion of the term involving the t^2/R in the stress-strain relations, reduced the above equations into the field equations of the linear extensional theory. The following set of equations is obtained:

Equilibrium Equations

$$\frac{\partial T_1}{\partial \alpha} - \frac{1}{R}\frac{\partial S_2}{\partial \beta} + \bar{X} = 0$$

$$\frac{\partial S_1}{\partial \alpha} + \frac{1}{R}\frac{\partial T_2}{\partial \beta} + \bar{Y} = 0$$

$$\frac{T_2}{R} + \bar{Z} = 0$$

$$\frac{\partial H_1}{\partial \alpha} - \frac{1}{R}\frac{\partial G_2}{\partial \beta} + N_2 + \bar{E} = 0$$

$$\frac{\partial G_1}{\partial \alpha} + \frac{1}{R}\frac{\partial H_2}{\partial \beta} - N_1 - \bar{F} = 0$$

Strain Displacement Equations

$$\epsilon_1 = \frac{\partial u}{\partial \alpha}$$

$$\epsilon_2 = \frac{1}{R}\left(\frac{\partial v}{\partial \beta} - w\right)$$

$$\epsilon_{12} = \frac{1}{R}\frac{\partial u}{\partial \beta} + \frac{\partial v}{\partial \alpha}$$

$$\kappa_1 = \frac{\partial^2 w}{\partial \alpha^2}$$

$$\kappa_2 = \frac{1}{R^2}\left(\frac{\partial^2 w}{\partial \beta^2} + \frac{\partial v}{\partial \beta}\right)$$

$$\kappa_{12} = \frac{1}{R}\left(\frac{\partial^2 w}{\partial \alpha\, \partial \beta} + \frac{\partial v}{\partial \alpha}\right)$$

Stress Strain Relations

$$T_1 = \frac{Et}{(1-\nu^2)}(\epsilon_1 + \nu\epsilon_2)$$

$$T_2 = \frac{Et}{(1-\nu^2)}(\epsilon_2 + \nu\epsilon_1)$$

$$S_1 = \frac{Et}{2(1+\nu)}(\epsilon_{12})$$

$$S_2 = -\frac{Et}{2(1+\nu)}(\epsilon_{12})$$

$$G_1 = -\frac{Et^3}{12(1-\nu^2)}(\kappa_1 + \nu\kappa_2)$$

$$G_2 = \frac{Et^3}{12(1-\nu^2)} \quad (\kappa_2 + \nu\kappa_1)$$

$$H_1 = \frac{Et^3}{12(1+\nu)} \quad (\kappa_{12})$$

$$H_2 = -\frac{Et^3}{12(1+\nu)} \quad (\kappa_{12})$$

Noticing from the stress-strain relations that $S_1 = -S_2$, and considering the fact that $\overline{X} = \overline{Y} = \overline{E} = \overline{F} = 0$, the first three equilibrium equations reduce to a system of three equations in three unknowns whose solution in terms of the integration functions to be determined from the boundary conditions are:

$$T_1 = -\frac{1}{R}\int_{a_1}^{a}\frac{\partial}{\partial\beta}\int_{a_1}^{a}\left(\frac{\partial\overline{Z}}{\partial\beta}\right)da\,da - \frac{1}{R}\int_{a_1}^{a}\frac{\partial}{\partial\beta}\,f_1(\beta)\,da + f_2(\beta)$$

$$T_2 = -R\,\overline{Z}$$

$$S_1 = \int_{a_1}^{a}\left(\frac{\partial\overline{Z}}{\partial\beta}\right)da + f_1(\beta)$$

The three strains then, following from the stress-strain relations, are of the form:

$$\epsilon_1 = -\frac{1}{ERt}\int_{a_1}^{a}\frac{\partial}{\partial\beta}\int_{a_1}^{a}\left(\frac{\partial\overline{Z}}{\partial\beta}\right)da\,da - \frac{1}{ERt}\int_{a_1}^{a}\frac{\partial}{\partial\beta}\,f_1(\beta)\,da + \frac{1}{Et}\,f_2(\beta) + \frac{\nu R}{Et}\,\overline{Z}$$

$$\epsilon_2 = -\frac{R}{Et}\,Z + \frac{\nu}{ERt}\int_{a_1}^{a}\frac{\partial}{\partial\beta}\int_{a_1}^{a}\left(\frac{\partial\overline{Z}}{\partial\beta}\right)da\,da + \frac{\nu}{ERt}\int_{a_1}^{a}\frac{\partial}{\partial\beta}\,f_1(\beta)\,da - \frac{\nu}{Et}\,f_2(\beta)$$

$$\epsilon_{12} = \frac{2(1+\nu)}{Et} \int_{a_1}^{a} \left(\frac{\partial \bar{Z}}{\partial \beta}\right) d\alpha + \frac{2(1+\nu)}{Et} f_1(\beta)$$

Having obtained these quantities, the strain-displacement relations can be integrated to give the following displacement in terms of the integration functions:

$$u = -\frac{1}{ERt} \int_{a_2}^{a} \int_{a_1}^{a} \frac{\partial}{\partial \beta} \int_{a_1}^{a} \left(\frac{\partial \bar{Z}}{\partial \beta}\right) d\alpha\, d\alpha\, d\alpha + \frac{\nu R}{Et} \int_{a_2}^{a} \bar{Z}\, d\alpha -$$

$$\frac{1}{ERt} \int_{a_2}^{a} \int_{a_1}^{a} \frac{\partial}{\partial \beta} f_1(\beta)\, d\alpha\, d\alpha + \frac{1}{Et} \int_{a_2}^{a} f_2(\beta)\, d\alpha + \phi_1(\beta)$$

$$v = \frac{2(1+\nu)}{Et} \int_{a_2}^{a} \int_{a_1}^{a} \left(\frac{\partial \bar{Z}}{\partial \beta}\right) d\alpha\, d\alpha + \frac{1}{ER^2 t} \int_{a_2}^{a} \int_{a_2}^{a} \frac{\partial}{\partial \beta} \int_{a_1}^{a} \frac{\partial}{\partial \beta} \int_{a_1}^{a} \left(\frac{\partial \bar{Z}}{\partial \beta}\right) d\alpha\, d\alpha\, d\alpha\, d\alpha -$$

$$\frac{\nu}{Et} \int_{a_2}^{a} \int_{a_2}^{a} \left(\frac{\partial \bar{Z}}{\partial \beta}\right) d\alpha\, d\alpha + \frac{2(1+\nu)}{Et} \int_{a_2}^{a} f_1(\beta)\, d\alpha + \frac{1}{ER^2 t} \int_{a_2}^{a} \frac{\partial}{\partial \beta} \int_{a_2}^{a} \int_{a_1}^{a} \frac{\partial}{\partial \beta} f_1(\beta)\, d\alpha\, d\alpha\, d\alpha -$$

$$\frac{1}{REt} \int_{a_2}^{a} \frac{\partial}{\partial \beta} \int_{a_2}^{a} f_2(\beta)\, d\alpha\, d\alpha - \frac{1}{R} \int_{a_2}^{a} \frac{\partial}{\partial \beta} \phi_1(\beta)\, d\alpha + \phi_2(\beta)$$

$$w = \frac{2(1+\nu)}{Et} \frac{\partial}{\partial \beta} \int_{a_2}^{a} \int_{a_1}^{a} \left(\frac{\partial \bar{Z}}{\partial \beta}\right) d\alpha\, d\alpha + \frac{1}{ER^2 t} \frac{\partial}{\partial \beta} \int_{a_2}^{a} \int_{a_2}^{a} \frac{\partial}{\partial \beta} \int_{a_1}^{a} \frac{\partial}{\partial \beta} \int_{a_1}^{a} \left(\frac{\partial \bar{Z}}{\partial \beta}\right) d\alpha\, d\alpha\, d\alpha\, d\alpha -$$

$$\frac{\nu}{Et} \frac{\partial}{\partial \beta} \int_{a_2}^{a} \int_{a_2}^{a} \left(\frac{\partial \bar{Z}}{\partial \beta}\right) d\alpha\, d\alpha + \frac{R^2}{Et} \bar{Z} - \frac{\nu}{Et} \int_{a_1}^{a} \frac{\partial}{\partial \beta} \int_{a_1}^{a} \left(\frac{\partial \bar{Z}}{\partial \beta}\right) d\alpha\, d\alpha +$$

$$\frac{2(1+\nu)}{Et}\ \frac{\partial}{\partial\beta}\int_{a_2}^{a} f_1(\beta)\,d\alpha + \frac{1}{ER^2t}\ \frac{\partial}{\partial\beta}\int_{a_2}^{a}\frac{\partial}{\partial\beta}\int_{a_2}^{a}\int_{a_1}^{a}\frac{\partial}{\partial\beta}\ f_1(\beta)\,d\alpha\,d\alpha\,d\alpha -$$

$$\frac{1}{ERt}\ \frac{\partial}{\partial\beta}\int_{a_2}^{a}\frac{\partial}{\partial\beta}\int_{a_2}^{a} f_2(\beta)\,d\alpha\,d\alpha - \frac{\nu}{Et}\int_{a_1}^{a}\frac{\partial}{\partial\beta}\ f_1(\beta)\,d\alpha +$$

$$\frac{\nu R}{Et}\ f_2(\beta) - \frac{1}{R}\ \frac{\partial}{\partial\beta}\int_{a_2}^{a}\frac{\partial}{\partial\beta}\ \phi_1(\beta)\,d\alpha + \frac{\partial}{\partial\beta}\ \phi_2(\beta)$$

This completes the solution of the fourth order system comprising the extensional theory of cylindrical shells. The constants of integration have to be evaluated from the boundary conditions. The bending and torsional moments can then be evaluated from the curvature - moment expressions of the stress-strain relations, after the evaluation of the curvatures, which were obtained by successive differentiation of the displacements with respect of the independent variables α and β. Having thus evaluated the bending and torsional moments, the transverse shears N_1 and N_2, that is, the quantities that were deleted from the equations of equilibrium in arriving at the extensional theory of shells, can now be evaluated from the fourth and fifth equilibrium equations. The validity of the extensional theory will be dependent upon the magnitude of these quantities since these were originally assumed to be negligent.

Analytical results for the meridional and circumferential strains and the radial displacement were determined, based on the following loading and boundary conditions:

Cylindrical Shell Completely Filled with Liquid Mercury

1) Loading

$\overline{Z} = A + B \cos\beta$, where

$A = -\gamma R = -4.864$ psi

$B = +\gamma R = +4.864$ psi

2) Boundary conditions

Measuring α from the mid-shell, the boundary conditions are:

$S_{1_{a=0}} = 0$

$u_{a=0} = 0$

$T_{1_{a=a_0}} = C + D \cos \beta$

$v_{a=a_0} = 0$, where (see appendix)

C +18.058 lb/in

D -24.077 lb/in

The boundary conditions imposed by the end plates were determined by taking into account not only the pressure exerted by the liquid mercury on the end plates and subsequently on the shell in the meridional direction, but also the effect of the resultant force due to mercury and the support rollers in creating an additional force distribution in the meridional direction at the end of the shell. This force system was created since the metal end plates were not counter weighted after the application of the mercury loading, since rollers are not perfectly frictionless when their axes are not normal to the axis of the cylindrical shell, and since it is not possible to place the support rollers at the surface of the inner edge of the end plate, thereby eliminating the eccentricity involved in the test setup. These conditions have been incorporated in the values of the constants in determining the boundary conditions.

In the ideal case of a frictionless support hinge involving no eccentricity and a perfectly counter weighted test setup, the boundary conditions, if the end plates are plane elastic plates, would be of the form $\bar{E} + \bar{F} \cos \theta$. In the case of a cylindrical shell completely filled with liquid mercury the constants $\bar{E}$ and $\bar{F}$ would assume, in this ideal case, the values $\frac{\gamma R^2}{2}$ and $-\frac{\gamma R^2}{4}$ respectively. However, the laboratory boundary conditions imposed were of the form $C + D \cos \beta$, thus incorporating the actual force system created at the laboratory.

Making use of the appropriate loading and the corresponding boundary conditions meridional and circumferential strains and radial displacements were evaluated at the midlength of the shell and at different circumferential points. The results, obtained through Avco RAD IBM 7094 Program No. 1406 based on reference 2, are presented in graphical form in figures 9 and 10.

The values for the quantities N_1 and N_2 were found to be of the order of 1 to 10,000 or less throughout the shell, assuring the applicability, as far as the analysis is concerned, of the linear extensional theory used in the case under consideration.

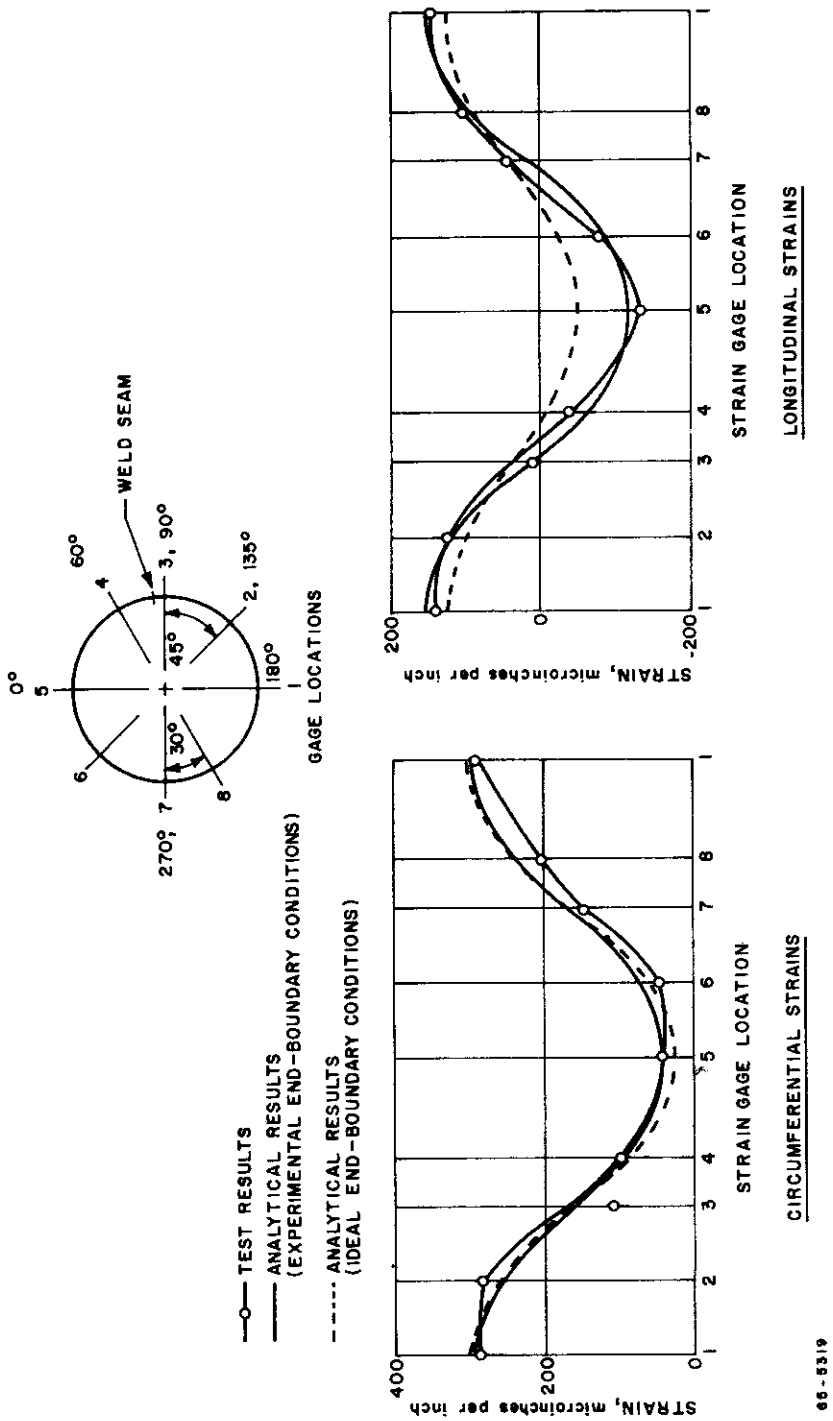

Figure 9 ANALYTICAL CIRCUMFERENTIAL AND LONGITUDINAL STRAINS COMPARED WITH EXPERIMENTAL STRAINS; CYLINDRICAL SHELL AT MIDLENGTH FILLED WITH LIQUID MERCURY AND AT ZERO PSI APPLIED INTERNAL PRESSURE

β DEGREES	ANALYTICAL W INCHES	EXPERIMENTAL W INCHES
0	0.00274	0.00400
30	0.00215	---
60	0.00055	0.00238
90	-0.00165	-0.00460
135	-0.00473	-0.00742
180	-0.00600	-0.00670
270	-0.00165	-0.00200

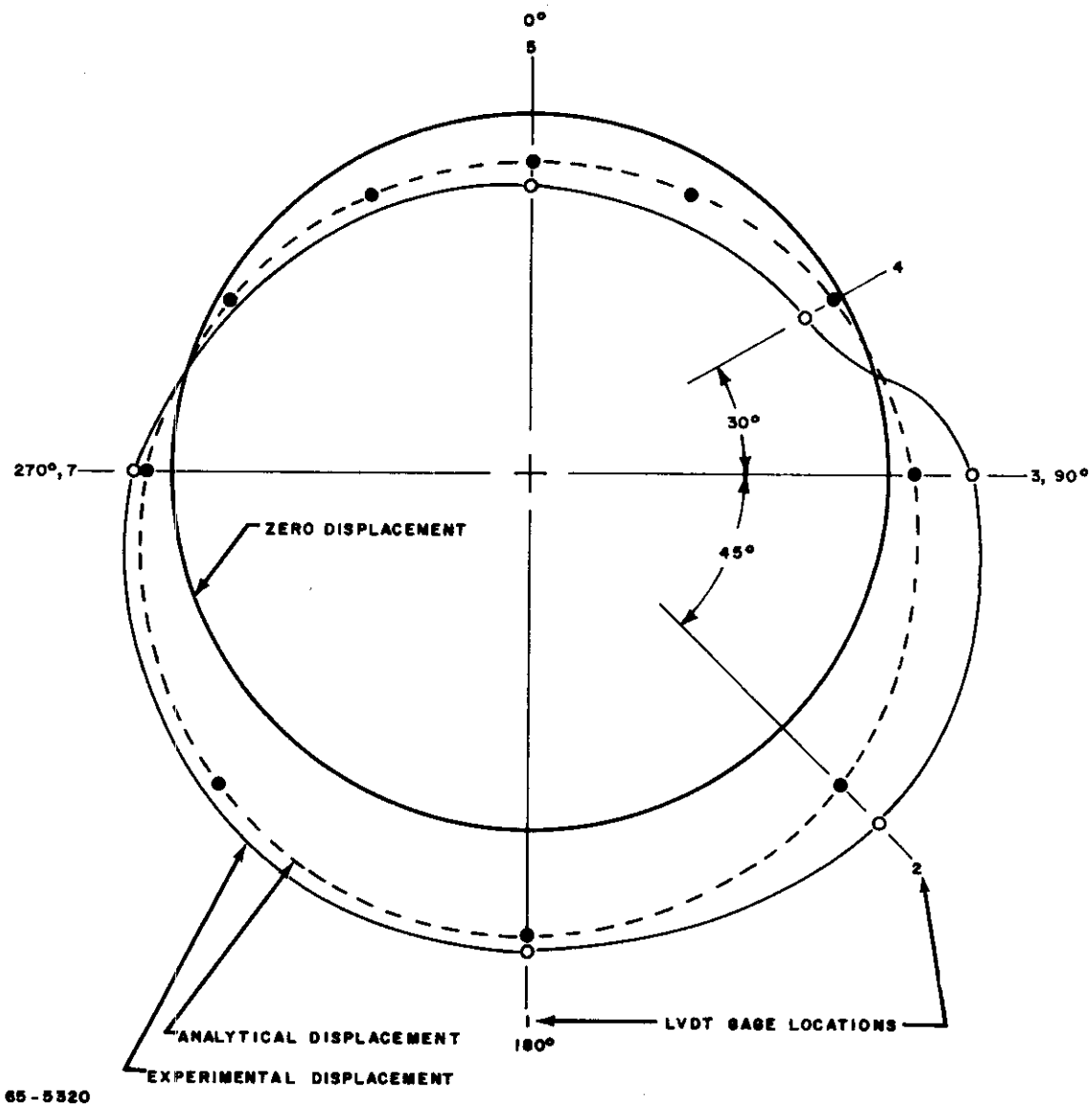

Figure 10 ANALYTICAL VERSUS EXPERIMENTAL RADIAL DISPLACEMENTS AT MIDLENGTH OF CYLINDRICAL SHELL FILLED WITH LIQUID MERCURY AND AT ZERO PSI APPLIED INTERNAL PRESSURE

3. Comparison of Experimental with Theoretical Results

Figure 9 shows plots of analytically obtained longitudinal and circumferential strains at mid-shell compared to the experimental points in the case of the cylindrical shell completely filled with liquid mercury and zero pressure. Figure 10 showing radial displacement, is an analogous plot to figure 9. Results are compared at the zero psi pressure rather than the maximum pressure of 28.2 psi because some permanent strain and deformation showed in the cylindrical shell at the 28.2 psi pressure level when repeated.

Figure 9 shows analytical results obtained for both ideal and laboratory-achieved boundary conditions (as mentioned in paragraph 2). As can be readily seen, the circumferential strains are not appreciably affected by the change in the boundary conditions. This is not so in the case of longitudinal strains. A careful review of the test setup after the application of the liquid mercury reveals the creation of an additional force system acting on the boundary of the cylindrical shell. An elementary free body diagram of the rod-plate assembly resting on the rollers accompanied by some analysis involving elementary statics (see appendix) shows plainly the creation of this additional force system. Under the boundary conditions imposed on the shell by this force system, the comparison of the meridional strains obtained analytically to the ones obtained experimentally are in good agreement. It is believed that if the analysis shown in the appendix was based on the true horizontal force developed at the rollers, and not on the analysis arrived at by assuming the value of μ, the agreement between theory and experiment would be much closer than that shown in figure 9.

The analytically obtained radial displacements shown in figures 10 agree very well with the experimentally obtained data, except in the 90 to 180 degree area. This obvious discrepancy is due to the weld bead (as would be expected) because of the pronounced stiffness of the shell in this area.

The structure behaved linearly with small deformations, substantiating the application of linear extensional theory in foil structures.

II. CONCLUSIONS

From the results obtained in this study, it can be concluded that linear extensional shell theory can be applied in the analysis of cylindrical shells under Newtonian pressure distribution, provided that the inplane boundary conditions are well defined. It is hoped that analogous studies involving unfurlable materials instead of foils can be carried out in the near future.

REFERENCES

1. Goldenveizer, A. L., Theory of Thin Elastic Shells, Permagon Press, 1961.

2. Lycurgus, N. C., Solution of Field Equations - Extensional Theory of Cylindrical Shells Under Arbitrary Non-Symmetrical Surface Loading Distribution, Avco RAD-TR-S220-T-46, 1962.

APPENDIX

Cylindrical Shell Completely Filled with Liquid Mercury. Boundary Conditions Incorporating Actual Force System at the Laboratory.

$$\overline{E} = \frac{\gamma R^2}{2} = 24.077 \text{ lb/in.}$$

$$\overline{F} = -\frac{\gamma R^2}{4} = -12.039 \text{ lb/in.}$$

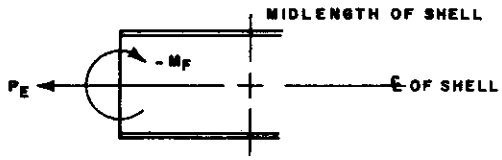

$$P_E = 2\pi R\overline{E} = 1497.685 \text{ lb.}$$

$$M_F = \pi R^2 \overline{F} = -3706.772 \text{ in-lb.}$$

Free body of cylindrical shell - Ideal boundary conditions on shell showing acting resultant forces

$$P = \pi R^2 (2\alpha_o)\gamma = 3055.886 \text{ lb.}$$

$$\frac{P}{2} = 1527.943 \text{ lb.}$$

$$e = 2.426 \text{ in.}$$

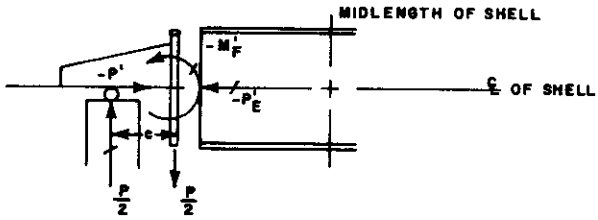

Assuming $\mu = 0.245$ we obtain

$$-P' = \left(\frac{P}{2}\right)\mu = 374.421 \text{ lb.}$$

Free body diagram - applied and reactive forces in Rod-Plate Assembly due to application of liquid mercury in the Cylindrical shell

$$M_F' = -\frac{P}{2}\, e = -3706.772 \text{ in.-lb}$$

$$P_E' = P' = -374.421 \text{ lb.}$$

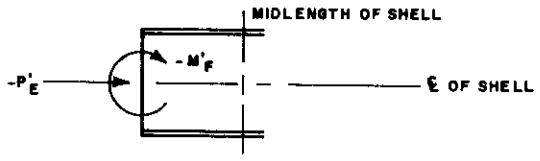

Additional induced force system in shell due to Laboratory Set-up

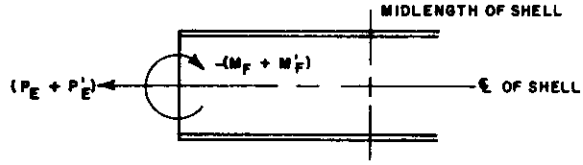

Total force system - ideal and induced - acting on shell boundary

Therefore

$$-(M_F + M_F') = 3706.772 + 3706.772 = 7413.544 \text{ in.-lb.}$$

$$(P_E + P_E') = 1497.685 - 374.421 = 1123.264 \text{ lb.}$$

$$C = \frac{(P_E + P_E')}{2\pi R} = +18.058 \text{ lb./in.}$$

$$D = \frac{(M_F + M_F')}{\pi R^2} = -24.077 \text{ lb./in.}$$

NOMENCLATURE

A	Fourier coefficient of the zero harmonic for the $\overline{Z}$ loading, psi
B	Fourier coefficient of the first harmonic for the $\overline{Z}$ loading, psi
C	Fourier coefficient of the zero harmonic of the boundary condition in T_1, actual force system, lb per in
D	Fourier coefficient of the first harmonic of the boundary condition in T_1, actual force system, lb per in
e	Distance between roller and inner face of circular plate, inches
E	Modulus of elasticity, psi
$\bar{E}$	Fourier coefficient of the zero harmonic of the boundary condition in T_1, ideal force system, lb per in
$\overline{E}$	External meridional bending moment, lb per in
$\bar{F}$	Fourier coefficient of the first harmonic of the boundary conditions in T_1, ideal force system, lb per in
$\overline{F}$	External circumferential bending moment, lb per in
G_1	Meridional bending moment, in-lb per in
G_2	Circumferential bending moment, in-lb per in
H_1	Meridional Torsional moment, in-lb per in
H_2	Circumferential torsional moment, in-lb per in
M_F	Overall resultant moment due to $\overline{F}$, in-lb
$M_{F'}$	Overall resultant moment due to $\frac{pe}{2}$, in-lb
N_1	Meridional transverse shear, lb per in
N_2	Circumferential transverse shear, lb per in
P	Resultant of mercury load, lb
P′	Force induced at rollers due to assumed coefficient of rolling-sliding friction, lb

NOMENCLATURE (Cont'd)

P_E	Overall resultant force due to $\overline{E}$, lb
P'_E	Overall resultant force due to P′, lb
R	Radius of cylindrical shell, in
S_1	Meridional inplane shear, lb per in
S_2	Circumferential inplane shear, lb per in
t	Thickness of cylindrical shell, in
T_1	Meridional stress resultant, lb per in
T_2	Circumferential stress resultant, lb per in
u	Meridional displacement, in
v	Circumferential displacement, in
w	Radial displacement, in
$\overline{X}$	Meridional surface loading on shell, psi
$\overline{Y}$	Circumferential surface loading on shell, psi
$\overline{Z}$	Normal surface loading on shell, psi
$f_1(\beta)$, $f_2(\beta)$, $\phi_1(\beta)$, $\phi_2(\beta)$	Integration functions to be determined from the boundary conditions
α	Meridional coordinate, in
α_o	Half length of cylindrical shell, in
α_1, α_2	Lower integration limits, fixed but of arbitrary choice
β	Circumferential coordinate, radians
γ	Density of mercury, lb per in^3
ϵ_1	Meridional extensional strain, in per in
ϵ_2	Circumferential extensional strain, in per in

NOMENCLATURE (Concl'd)

ϵ_{12}	Inplane shearing strain, in per in
κ_1	Meridional bending strain, per in
κ_2	Circumferential bending strain, per in
κ_{12}	Torsional strain, per in
μ	Coefficient of rolling-sliding friction, dimensionless
ν	Poisson's ratio, dimensionless